

Article

Effects of the Novel Triazole Fungicide Ipfentrifluconazole on Different Endpoints in Zebrafish Larvae

Mingfei Xu ¹, Yilin Huang ², Mingrong Qian ³, Yuanxiang Jin ^{2,*}  and Hu Zhang ^{1,*}

¹ Institute of Agro-Product Safety and Nutrition, Zhejiang Academy of Agricultural Sciences, Hangzhou 310021, China

² College of Biotechnology and Bioengineering, Zhejiang University of Technology, Hangzhou 310014, China

³ Key Laboratory of Pollution Exposure and Health Intervention of Zhejiang Province, Interdisciplinary Research Academy, Zhejiang Shuren University, Hangzhou 310015, China

* Correspondence: jinyx@zjut.edu.cn (Y.J.); zhanghu@mail.zaas.ac.cn (H.Z.)

Abstract

The potential hazards of triazole fungicides to non-target organisms necessitate environmental risk assessment. This study, therefore, focused on characterizing the differential toxicity of the enantiomers of Ipfentrifluconazole (IFZ), a new triazole fungicide, in zebrafish larvae using a multi-endpoint approach. Acute toxicity tests determined the LC₅₀ values of 1.709 mg/L for rac-IFZ, 1.531 mg/L for (+)-IFZ, and 1.809 mg/L for (–)-IFZ, indicating a higher toxicity of the (+)-enantiomer. To avoid overt mortality while revealing organ-level effects, we chose a concentration of approximately 20% of the LC₅₀ of (+)-IFZ, which is 340 µg/L, as the exposure concentration. Exposure to IFZ induced developmental defects, including swim bladder malformation, cardiac blood pooling, and metabolic disturbances during the early developmental stage of zebrafish. Additionally, cardiac and hepatic development and function were disrupted in zebrafish larvae following IFZ exposure. Biochemical and transcriptomic analyses revealed distinct toxic mechanisms: (+)-IFZ primarily disrupted lipid metabolism through alterations in PPAR signaling pathway and fatty acid degradation, while (–)-IFZ significantly impaired cardiac function by affecting adrenergic signaling in cardiomyocytes and cardiac muscle contraction. Rac-IFZ mainly influenced drug metabolism, particularly cytochrome P450-related pathways. These findings demonstrated the toxic effects of IFZ, emphasizing the need for evaluating environmental and health risks of chiral pesticides. The study provides valuable insights into the molecular mechanisms underlying IFZ toxicity.

Keywords: Ipfentrifluconazole; transcriptomics; zebrafish larvae



Academic Editor: Carlos Barata

Received: 1 September 2025

Revised: 23 September 2025

Accepted: 27 September 2025

Published: 29 September 2025

Citation: Xu, M.; Huang, Y.; Qian, M.; Jin, Y.; Zhang, H. Effects of the Novel Triazole Fungicide Ipfentrifluconazole on Different Endpoints in Zebrafish Larvae. *Toxics* **2025**, *13*, 830. <https://doi.org/10.3390/toxics13100830>

Copyright: © 2025 by the authors. Licensee MDPI, Basel, Switzerland. This article is an open access article distributed under the terms and conditions of the Creative Commons Attribution (CC BY) license (<https://creativecommons.org/licenses/by/4.0/>).

1. Introduction

Triazole fungicides represent a significant category of agrochemicals extensively employed in farming to manage diverse fungal infections. Owing to their high efficacy, broad-spectrum activity and low toxicity, triazole fungicides are vital in modern agriculture [1]. Triazole fungicides usually have a triazole ring structure, which gives them unique fungicidal activity. This class of fungicides mainly interferes with the biosynthesis of fungal cell membranes by inhibiting sterol demethylase, thereby inhibiting the growth and reproduction of fungi [2]. Since the advent of the first triazole fungicide, triadimefon, in the 1970s, triazole fungicides have experienced rapid development. Subsequently, a series of new triazole fungicides with high efficiency and low toxicity have been developed, such as Flusilazole, Tebuconazole, Epoxiconazole, etc. [3]. The extensive application of triazole

fungicides has led to rising awareness of their ecological consequences, particularly regarding non-target organisms like zebrafish. Studies have shown that triazole fungicides can cause adverse effects in zebrafish, manifested as abnormal behavior, decreased swimming ability [4], and even death [5]. Triazole fungicides can induce oxidative stress in zebrafish, leading to cell and DNA damage. Some triazole fungicides can act as endocrine disruptors in zebrafish, altering their hormonal balance and consequently impairing reproductive system function [6].

Ipfentrifluconazole (IFZ) is a new triazole fungicide developed by BASF in recent years. It contains an asymmetric chiral carbon atom and is composed of a pair of enantiomers. IFZ functions by disrupting ergosterol production in pathogenic organisms, compromising cellular membrane integrity. This interference impedes critical fungal structures including attachment cells, haustoria, hyphal growth, and spore formation. However, investigations into IFZ's ecological consequences for aquatic systems and non-target species remain notably limited. However, mefentrifluconazole (MFZ), which only differs from IFZ in its chemical structure by methyl and isopropyl, has been widely studied by researchers. Studies have shown that MFZ exposure can cause *Eisenia fetida* cell membrane damage and apoptosis, and the selectivity of apoptosis may be dominated by the mitochondrial pathway. Comparative studies reveal distinct bioactivity between the MFZ stereoisomers. The S-(+)-enantiomer demonstrates specific upregulation of mitochondrial structural components, resulting in exacerbated mitochondrial fragmentation. More significantly, this isomer potently disrupts bioenergetic processes through dual inhibition of mitochondrial respiratory chain complexes I (NADH dehydrogenase) and IV (cytochrome c oxidase), thereby impairing electron flux and ATP generation capacity to a greater extent than its R-(−)-counterpart [7]. In addition, experimental evidence demonstrates that MFZ exposure induces enantioselective developmental toxicity in zebrafish across multiple organ systems. Cardiac manifestations include embryonal bradycardia, pericardial and yolk sac deformities, and significant downregulation of cardiac-specific genetic markers. Concurrently, neurodevelopmental impacts are observed through suppressed spontaneous movements, altered locomotor activity such as swimming speed and distance, and modulated expression of neurotoxicity-related genes. These effects consistently show stereochemical dependence, with enantiomers exhibiting enhanced bioactivity [8]. In addition, MFZ also causes enantioselective changes in the metabolomics of adult zebrafish livers [9], and MFZ exposure impairs liver structure and liver lipid metabolism in mice, impairs intestinal barrier function, and promotes inflammation [10]. Therefore, it is of significance to explore whether IFZ has similar toxic effects to MFZ or whether it has unique toxic effects.

The zebrafish (*Danio rerio*) has become a widely adopted and instrumental model organism for toxicological research, particularly for assessing the safety of pesticides, environmental contaminants, and pharmaceuticals. With approximately 70% genetic homology to humans and conserved core physiological pathways, zebrafish exhibit remarkable similarities to mammalian systems. Zebrafish exhibit significant structural and functional conservation in their hepatic, renal, and cardiovascular systems when compared to mammals. This high degree of homology establishes the zebrafish as a powerful and versatile model organism for studying the mechanisms of chemical toxicity and for evaluating the physiological effects of toxicants [11]. Zebrafish embryos and larvae are transparent in the early stages of development, and processes such as organ formation, blood circulation, and cell apoptosis can be directly observed under a microscope. This feature makes it an ideal model for studying developmental toxicity, teratogenicity, and cardiotoxicity [12]. In addition, zebrafish have the characteristics of strong reproductive capacity and rapid embryonic development, which is suitable for high-throughput toxicity screening [13].

This study first explored the effects of IFZ on the growth and development of zebrafish embryos. Then, we explored the effects of IFZ on the development and function of the heart and liver of zebrafish larvae. Finally, the transcriptomic analysis was used to analyze the selective effects of IFZ racemates and enantiomers. At present, there is a lack of research on the effects of IFZ on the growth and development of zebrafish and the functions of various organs. This study will provide some theoretical basis for the toxicological effects of IFZ.

2. Materials and Methods

2.1. Chemicals

Ipfentrifluconazole (IFZ) (CAS No:1417782-08-1) was purchased from Altascientific (Tianjin, China). The enantiomers were separated according to the research method reported by Li et al. [14]. IFZ was dissolved in dimethyl sulfoxide (DMSO) and subsequently stored at $-20\text{ }^{\circ}\text{C}$ to maintain stability until required for experiments.

2.2. Zebrafish Breeding and Embryo Collection

This study employed wild-type zebrafish alongside two transgenic models, *Tg(myl7:EGFP)* and *Tg(-1.7apoa2:GFP)*, which were obtained from the China Zebrafish Resource Center in Wuhan. All zebrafish were housed in glass aquarium systems supplied with activated carbon-filtered and dechlorinated tap water, maintained at $28 \pm 1\text{ }^{\circ}\text{C}$. The facility maintained a 14 h light/10 h dark photoperiod to regulate circadian rhythms. For nutritional requirements, the zebrafish received feedings of freshly hatched brine shrimp twice each day. Breeding protocols involved placing adult zebrafish in specialized mating tanks overnight at a ratio of two females to one male. The following morning, spawning was induced through partition removal between the sexes, with subsequent embryo collection completed within a 30 min window followed by rinsing to prepare for experimental procedures.

2.3. Detection of Acute Toxicity

The acute toxicity of IFZ to zebrafish embryos was evaluated according to OECD Test Guideline No. 236. The exposure period spanned from 2 h post-fertilization (hpf) to 96 hpf. In preliminary tests, six IFZ concentrations (400, 800, 1200, 1600, 2000, and 2400 $\mu\text{g/L}$) were examined. For each concentration, 30 fertilized embryos were transferred into six-well plates containing 5 mL of exposure solution, with three replicates per group. The exposure solution was renewed every 24 h. During the experimental period, culture plates were covered to minimize solvent evaporation and maintained in an incubator at a constant $28\text{ }^{\circ}\text{C}$ under a 14/10 h light/dark photoperiod. All tests were initiated at 2 h post-fertilization (2 hpf) using non-dechlorinated embryos. Daily observations included recording hatching success and mortality rates. For data analysis, IFZ concentrations were \log_{10} -transformed and plotted on the x-axis, while mortality rates were represented on the y-axis. A dose–response curve was generated using nonlinear regression to estimate the median lethal concentration (LC_{50}).

Based on the LC_{50} values of IFZ obtained from the experiments above, an exposure concentration of 340 $\mu\text{g/L}$ was chosen. Stock solutions of both the racemate and the separate enantiomers were prepared and then diluted using E3 medium to reach the target concentration of 340 $\mu\text{g/L}$. Four experimental groups were established: Control (CON), rac-IFZ (rac), (+)-IFZ (+), and (–)-IFZ (–). The CON group served as the DMSO solvent control, with DMSO levels in all test solutions kept at or below 0.1% (*v/v*). For each experimental condition, a total of 120 embryos were carefully transferred into individual glass beakers, each containing 200 mL of the designated test solution. The larvae were maintained under a constant temperature of $28\text{ }^{\circ}\text{C}$ and a photoperiod of 14 h light and 10 h

darkness. Every 24 h, three-quarters of the test medium was refreshed. Following 7 days of continuous exposure, zebrafish larvae were gathered for further analysis.

2.4. Biochemical Indicators Analysis

The tissue samples were first homogenized in phosphate-buffered saline (PBS) and subsequently subjected to centrifugation at 4000 rpm for a duration of 10 min under 4 °C to isolate the supernatant. A precise 20 µL aliquot of the resulting clear upper phase was then carefully collected from each processed sample. Total protein content was quantified using a BCA Protein Assay Kit (Sangon, Shanghai, China). Furthermore, key metabolic biomarkers, including triglyceride, total cholesterol, glucose, and pyruvate, were assessed employing commercial enzymatic assay kits (Nanjing Jiancheng Bioengineering Institute, Nanjing, China) in strict accordance with the manufacturer's protocols.

2.5. RNA Extraction and Transcriptome Analysis

Total RNA isolation was performed with TRIZOL reagent (Vazyme, Nanjing, China), and RNA integrity was assessed using the RNA Nano 6000 Assay Kit on an Agilent Bioanalyzer 2100 system (Agilent Technologies, Santa Clara, CA, USA). Sequencing libraries were prepared with the NEBNext[®] Ultra[™] RNA Library Prep Kit (NEB, Ipswich, MA, USA), and their quality was evaluated via the Qubit[®] 2.0 Fluorometer (Thermo Fisher Scientific, Waltham, MA, USA) as well as quantitative real-time PCR (qRT-PCR). Cluster generation was carried out on the Illumina cBot system (Illumina, Inc., San Diego, CA, USA) with the TruSeq PE Cluster Kit v3-cBot-HS (Illumina, Inc., San Diego, CA, USA), and the libraries were subsequently sequenced on the Illumina NovaSeq platform (Illumina, Inc., San Diego, CA, USA) to generate 150 bp paired-end reads. Raw sequencing data were preprocessed by eliminating adapter sequences, low-quality reads, and poly-N segments using in-house Perl scripts. Differential gene expression analysis was performed using DESeq2 version 1.20.0, with differentially expressed genes identified based on an adjusted *p*-value cutoff of less than 0.05 after the Benjamini–Hochberg correction. Significant genes were functionally annotated using Gene Set Enrichment Analysis (GSEA) and KEGG pathway analysis, both performed with the clusterProfiler package in R 4.3.1.

2.6. Gene Expression Analysis

All experimental conditions were analyzed with six independent biological replicates, with each replicate consisting of 30 zebrafish larvae. Total RNA was isolated with TRIZOL reagent (Vazyme, Nanjing, China), and complementary DNA (cDNA) was synthesized through reverse transcription. Quantitative real-time PCR (qPCR) was subsequently carried out using a SYBR Green master mix (Vazyme, Nanjing, China) on a Bio-Rad CFX Connect Real-Time PCR Detection System. The *eflα* gene was used as an endogenous control for data normalization, and the relative expression levels of the genes of interest were determined based on the comparative threshold cycle ($2^{-\Delta\Delta CT}$) method. The loop conditions and relative gene expression follow the previously established protocol [15,16].

2.7. Observation of Heart Morphology of Tg(*myl7*: EGFP)

To assess cardiac development, embryos were distributed into six-well plates with 30 embryos per well. The embryos were continuously exposed for 96 h. Afterwards, 10 randomly selected larvae were observed under a fluorescence microscope for cardiac morphology and related cardiac parameters were measured. Zebrafish were photographed at the end of ventricular systole and at the end of ventricular diastole, and the software

ImageJ-win32 was used to quantify the ventricular areas at the end of systole and diastole. The formulas for calculating stroke volume and ejection fraction were as follows:

$$\text{stroke volume} = \text{VEDA} - \text{VESA}$$

$$\text{ejection fraction} = (\text{stroke volume})/\text{VEDA}$$

$$\text{fractional shortening} = (\text{Dd} - \text{Ds})/\text{Dd}$$

VEDA: Ventricular end-diastolic area.

VESA: Ventricular end-systolic area.

Dd: Ventricular end-diastolic diameter.

Ds: Ventricular end-systolic diameter.

2.8. Observation of Liver Morphology of *Tg(-1.7apoa2: GFP)*

Ten larval zebrafish (96 hpf) were randomly selected to observe the liver development. Thirty embryos were placed in each well of a six-well plate, and after 7 consecutive days of exposure, the liver morphology was observed under a microscope and the liver area and fluorescence intensity of the liver region were measured.

2.9. Statistical Analysis

All statistical analyses were conducted using GraphPad Prism version 8.0. Results were presented as mean \pm SEM. Group comparisons were carried out by one-way ANOVA, with asterisks (*) used to mark significant differences compared to the control group (* $p < 0.05$, ** $p < 0.01$), and hashtags (#) indicating significant differences between experimental treatments (# $p < 0.05$).

3. Results

3.1. Developmental Toxicity of IFZ to Zebrafish Larvae

This study evaluated the acute toxic effects of IFZ on zebrafish larvae following a 96 h exposure period across a gradient of concentrations, during which mortality was systematically documented. The calculated LC₅₀ values were 1.709 mg/L for rac-IFZ, 1.531 mg/L for (+)-IFZ, and 1.809 mg/L for (–)-IFZ (Figure 1A). Subsequent morphological observations on days 4 and 7 revealed incomplete swim bladder development in IFZ exposure larvae, along with evident blood pooling in the cardiac region. These findings suggested potential impairment of heart development or possible thrombotic events (Figure 1B). Next, the TC, TG, glucose, and pyruvate levels were measured. The results indicated a significant increase in triglyceride (TG) content following IFZ exposure. The TC and glucose contents in the (–)-IFZ group also increased significantly (Table 1). Moreover, the expression levels of mRNA linked to glucose and lipid metabolism, along with apoptosis-related genes, were quantitatively assessed. The findings revealed that IFZ exposure disrupted glucose metabolism and triggered apoptosis in the larvae, with the (–)-IFZ isomer exerting a more pronounced effect. Both (+)-IFZ and (–)-IFZ treatments affected the lipid metabolism of zebrafish larvae (Figure 1C).

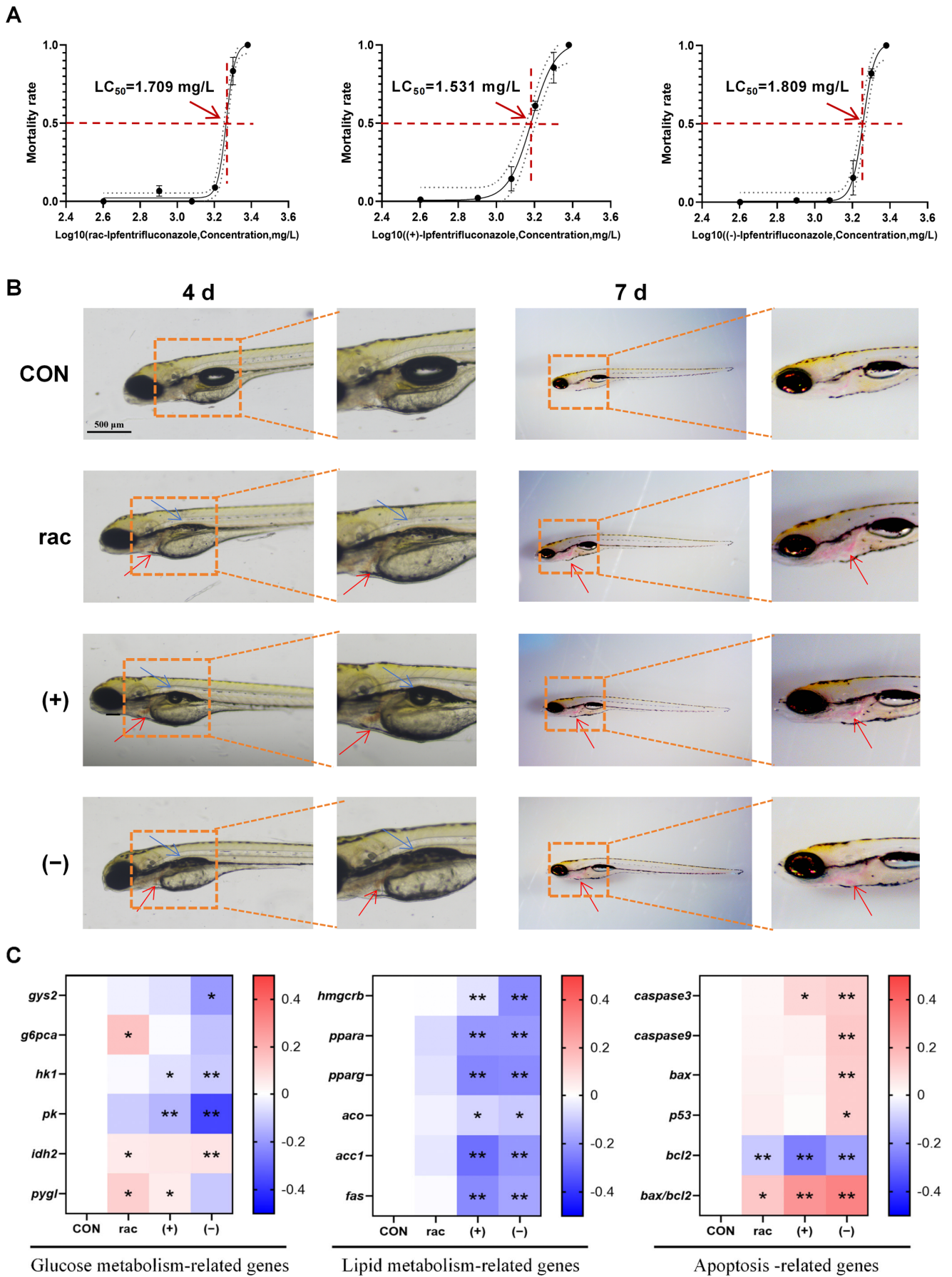


Figure 1. Developmental toxicity of IFZ to zebrafish larvae. (A) Semi-mortality curve of zebrafish larvae exposed to different concentrations at 4 d. (B) Morphological images of larval zebrafish at 4 d

and 7 d. The blue arrows indicate abnormal swim bladder development while the red arrows indicate blood pooling in the pericardial area. (C) The mRNA levels of genes related to glucose and lipid metabolism and apoptosis ($n = 6$). Data are presented as the mean \pm SEM. Asterisks indicate significant difference between treatment group and control (* $p < 0.05$; ** $p < 0.01$).

Table 1. Effects of Ipfentrifluconazole exposure on the biochemical indicators of zebrafish larvae.

Biochemical Indicators	Ipfentrifluconazole			
	CON	Rac-Ipfentrifluconazole	(+)-Ipfentrifluconazole	(-)-Ipfentrifluconazole
TG (mmol/gprot)	0.016 \pm 0.001	0.023 \pm 0.001 **	0.028 \pm 0.001 **	0.024 \pm 0.000 **
TC (mmol/gprot)	0.083 \pm 0.002	0.087 \pm 0.001	0.089 \pm 0.002	0.098 \pm 0.003 **
Glucose (mmol/gprot)	0.086 \pm 0.003	0.084 \pm 0.002	0.091 \pm 0.003	0.099 \pm 0.003 *
Pyruvate (mmol/gprot)	0.027 \pm 0.003	0.026 \pm 0.002	0.025 \pm 0.002	0.024 \pm 0.001

Full name of biochemical indicators: TG, total triglycerides; TC, total cholesterol. The presented values are the mean \pm SEM ($n = 6$), * $p < 0.05$; ** $p < 0.01$ versus control group.

3.2. Cardiotoxicity of IFZ to Zebrafish Larvae

Since obvious abnormalities were found in the heart area of the larvae in the IFZ treatment group when observing the morphology of the larvae on the 4th and 7th days, the transgenic larvae *Tg(myl7: EGFP)* were used to observe the heart morphology and measure heart-related indicators. As demonstrated in Figure 2A,B, IFZ exposure significantly elevated larval heart rate while reducing stroke volume. Notably, (+)-IFZ treatment additionally increased ventricular end-systolic area and decreased shortening fraction. (-)-IFZ exposure significantly reduced larval ejection fraction. Subsequent analysis of cardiovascular-related gene expression revealed significant alterations in mRNA levels for both (+)-IFZ and (-)-IFZ treatment groups (Figure 2C).

3.3. Hepatotoxicity of IFZ to Zebrafish Larvae

Building upon the observed lipid metabolic disruptions, we employed *Tg(-1.7apoa2:GFP)* zebrafish to assess hepatotoxicity (Figure 3A). IFZ exposure universally increased hepatic area and GFP fluorescence intensity, with rac-IFZ and (+)-IFZ showing particularly pronounced hepatomegaly (Figure 3B). Molecular analysis revealed enantiomer-specific oxidative stress responses, where (+)-IFZ induced the most substantial alterations in oxidative stress-related gene expression profiles (Figure 3C).

3.4. Transcriptomic Analysis of IFZ Exposed to Larval Zebrafish

To elucidate the molecular mechanisms underlying IFZ toxicity, we conducted transcriptome profiling of exposed zebrafish. Quality control assessment demonstrated strong reproducibility, as evidenced by hierarchical clustering where biological replicates from each treatment group formed distinct clusters in the heatmap analysis. This consistent grouping pattern confirmed the reliability of our transcriptional data for subsequent differential expression analysis (Figure 4A). The results in Figure 4B,C showed that the rac-IFZ treatment group had 423 differentially expressed genes (DEGs), the (+)-IFZ treatment group had 558 DEGs, while the (-)-IFZ treatment group had 890 DEGs and had the largest number of up-regulated and down-regulated genes (Figure 4B,C). Principal component analysis revealed that all treatment groups were distinctly clustered and separated from the control cohort. Notably, the (-)-IFZ group was the most removed from the control, underscoring its pronounced differential effect (Figure 4D). Subsequent KEGG pathway enrichment analysis of these DEGs identified significant involvement in processes includ-

ing drug metabolism, cardiac development, lipid metabolism, apoptosis, and autophagy (Figure 4E).

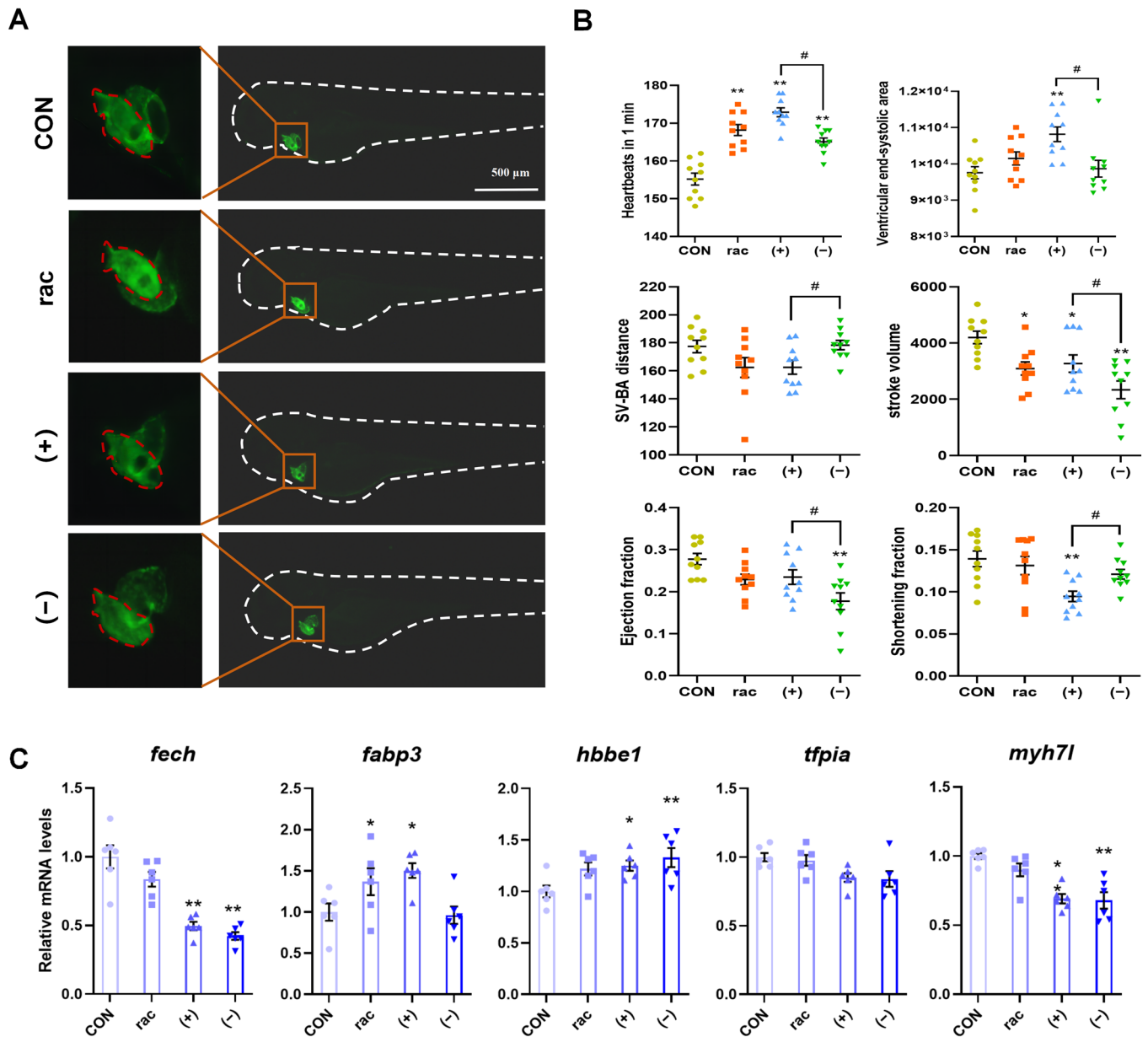


Figure 2. Cardiotoxicity of IFZ to zebrafish larvae. (A) Heart morphology of *Tg(myl7: EGFP)* transgenic zebrafish. (B) Determination of heart-related indicators ($n = 10$). (C) mRNA levels of cardiac development and function-related genes ($n = 6$). Data are presented as the mean \pm SEM. Asterisks indicate significant difference between treatment group and control ($* p < 0.05$; $** p < 0.01$). Hashtags indicate significant difference between different treatment groups ($\# p < 0.05$).

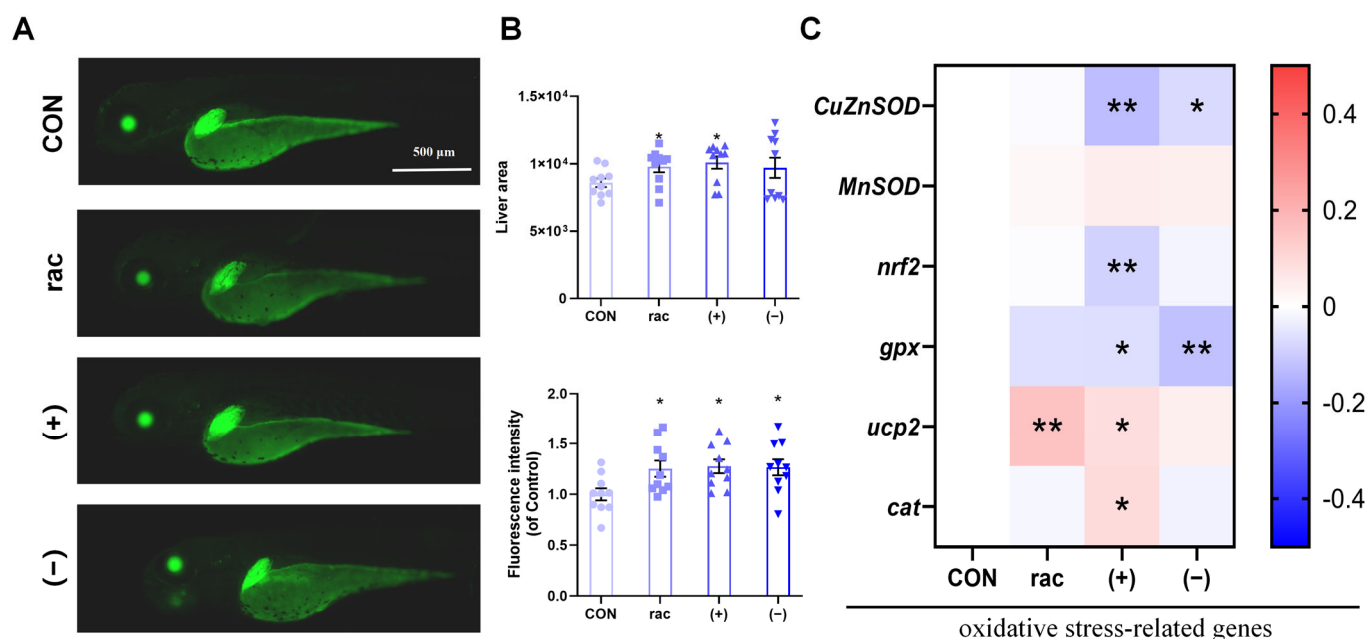


Figure 3. Hepatotoxicity of IFZ to zebrafish larvae. (A) Liver morphology of *Tg(-1.7apoa2: GFP)* transgenic zebrafish. (B) Quantification of larval liver area and fluorescence intensity ($n = 10$). (C) The mRNA levels of oxidative stress-related genes ($n = 6$). Data are presented as the mean \pm SEM. Asterisks indicate significant difference between treatment group and control (* $p < 0.05$; ** $p < 0.01$).

3.5. Comparison of Transcriptomes Between Racemates and Enantiomers of IFZ

To further explore the differences between racemates and enantiomers, the DEGs in each group were compared using a Venn diagram, and then the DEGs specific to each treatment group were subjected to KEGG enrichment analysis. Consistent with the volcano plot analysis, the (–)-IFZ treatment group exhibited the highest number of unique DEGs. Functional enrichment analysis revealed these DEGs were predominantly associated with cardiac development and function pathways, including adrenergic signaling in cardiomyocytes, apelin signaling pathway and cardiac muscle contraction (Figure 5B). Transcriptomic profiling revealed significant enrichment of lipid metabolism pathways in (+)-IFZ-exposed zebrafish, with the PPAR signaling pathway showing particularly strong activation. Additional affected metabolic processes included fatty acid degradation and biosynthesis pathways, suggesting disruption of lipid homeostasis (Figure 5A). The rac-IFZ treatment group exhibited the fewest unique DEGs, with pathway enrichment analysis revealing predominant involvement in xenobiotic metabolic processes, particularly cytochrome P450-mediated pathways including metabolism of xenobiotics by cytochrome P450, drug metabolism-cytochrome P450 and other drug-metabolizing enzyme systems (Figure 5C). Additionally, KEGG pathway enrichment analysis was conducted on the DEGs common to all three treatment groups. The findings revealed significant enrichment in key biological pathways, including cardiac adrenergic signaling, autophagy regulation, and mitophagy processes (Figure 5D).

To further investigate the distinctions between IFZ enantiomers, we conducted KEGG enrichment analysis on the DEGs comparing the (+)-IFZ and (–)-IFZ treatment groups, with the (–)-IFZ group serving as the control. This analysis identified significant enrichment in pathways related to lipid metabolism, cardiac development, and cardiac function (Figure 5E). Subsequently, GSEA was performed focusing on the fatty acid degradation, PPAR signaling pathway, adrenergic signaling in cardiomyocytes, and cardiac muscle contraction. The results demonstrated a marked upregulation of these four pathways in the (+)-IFZ group relative to the (–)-IFZ group (Figure 5F).

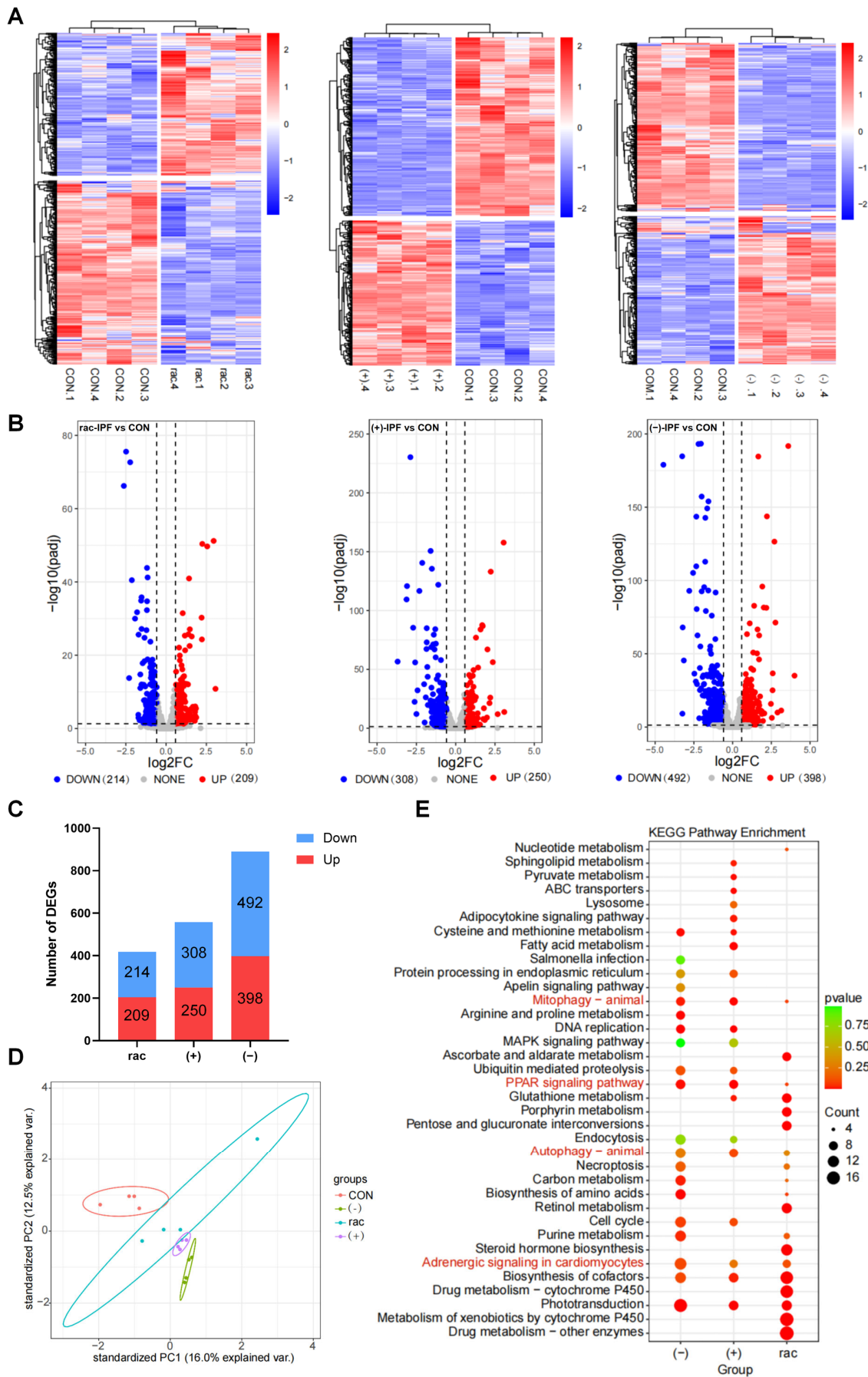


Figure 4. Transcriptomic analysis of IFZ exposed to larval zebrafish. (A) Heatmap of cluster analysis using fpkm of differentially expressed genes (DEGs). (B) Volcano map based on DEGs ($p < 0.05$ and

fold change > 1.5). (C) The number of DEGs in each treatment group. (D) Principal component analysis (PCA). (E) Enrichment analysis of KEGG pathway map based on all DEGs.

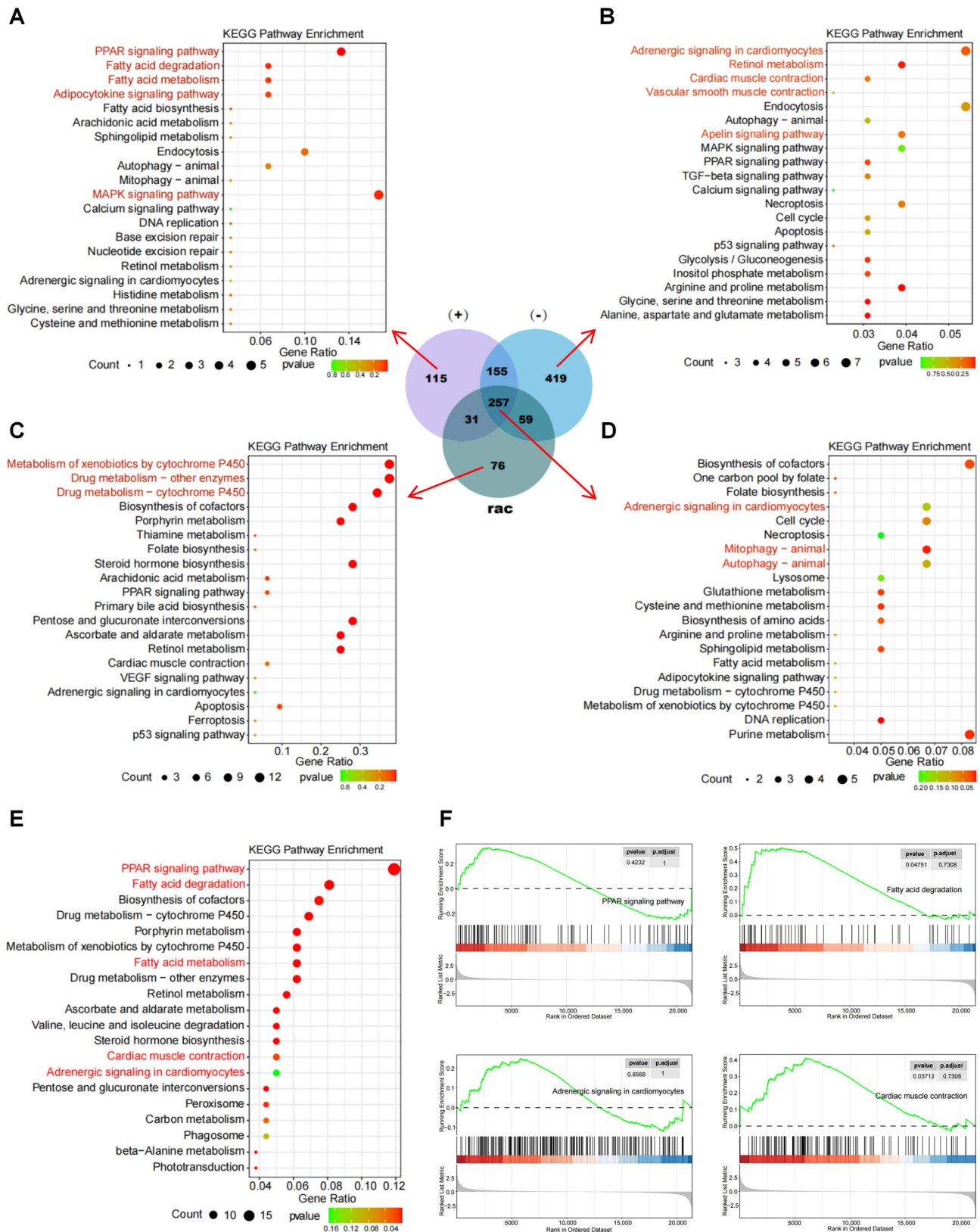


Figure 5. Comparison of transcriptomes between racemates and enantiomers of IFZ. Enrichment analysis of KEGG pathway map based on DEGs unique to the (+)-IFZ group (A), (-)-IFZ group (B), and rac-IFZ group (C). (D) Enrichment analysis of KEGG pathway map based on common DEGs across all three treatment groups. (E) Enrichment analysis of KEGG pathway map based on DEGs

between (+)-IFZ and (-)-IFZ groups. (F) GSEA analysis of PPAR signaling pathway, fatty acid degradation, adrenergic signaling in cardiomyocytes, and cardiac muscle contraction.

To verify the transcriptome results, five DEGs linked to adrenergic signaling in cardiomyocytes and the PPAR signaling pathway were chosen for validation via RT-qPCR. The experimental results demonstrated consistent expression patterns with the transcriptome fpkm values, thereby confirming the reliability of the RNA-seq data (Figure 6).

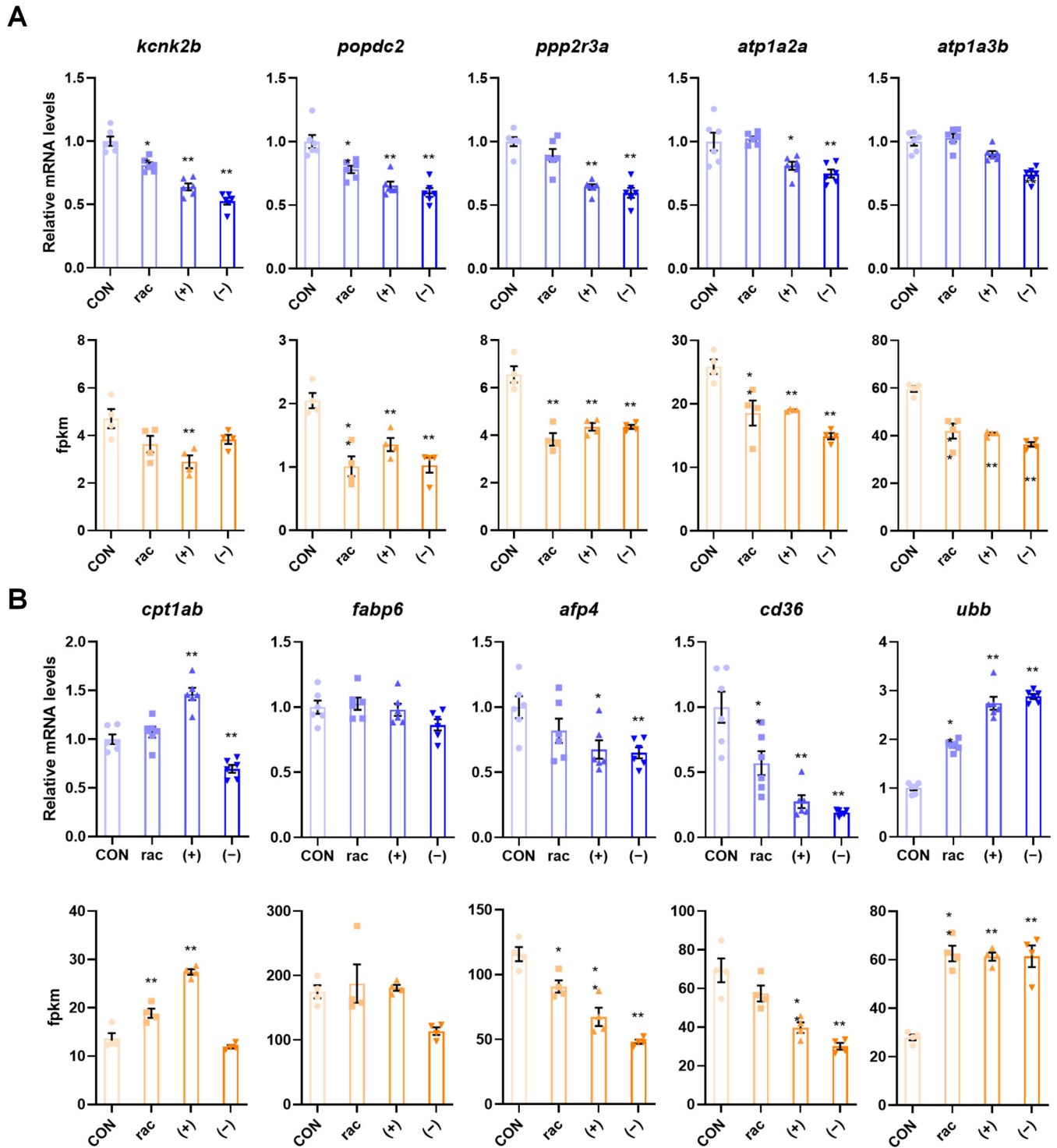


Figure 6. Validation of transcriptomic results. (A) Five genes associated with adrenergic signaling in cardiomyocytes were verified using qRT-PCR and verified using the fpkm values in the transcriptome data. (B) Five genes associated with PPAR signaling pathway were verified using qRT-PCR ($n = 6$) and verified using the fpkm values ($n = 4$) in the transcriptome data. Data are presented as the mean \pm SEM.

Asterisks indicate a significant difference between treatment group and control (* $p < 0.05$; ** $p < 0.01$).

4. Discussion

Triazole fungicides are a class of highly effective and broad-spectrum organic heterocyclic fungicides. They inhibit 14α -demethylation reactions mediated by fungal cytochrome P450 (CYP51), block ergosterol synthesis, and thus destroy cell membrane structures and exert antibacterial effects [17]. Nevertheless, their possible adverse effects on non-target species have raised growing concerns. Research indicates that triazole compounds can disrupt steroid hormone metabolism, potentially causing endocrine dysfunction through inhibition of key mammalian CYP450 enzymes, including CYP19 and CYP17 [18]. Previous studies have identified that several triazole fungicides, including tebuconazole and propiconazole, can induce excessive production of reactive oxygen species (ROS). This oxidative burst leads to cellular oxidative stress and subsequent DNA damage, ultimately contributing to genomic instability. These effects may potentially disrupt embryogenesis and exhibit teratogenic properties [2,19]. Their environmental persistence and bioaccumulation further increase ecotoxicological risks. As a new type of triazole fungicide, IFZ has relatively few studies on its toxicological effects. Therefore, a comprehensive investigation into the molecular toxicological mechanisms of IFZ is essential for assessing its potential risks to environmental safety and human health.

The median lethal concentration (LC_{50}) serves as a fundamental indicator for evaluating acute toxicity, specifically measuring the short-term lethal effects of triazole fungicides on zebrafish larvae. This well-established parameter offers critical insights into the immediate toxicological potential of chemical compounds [20]. In this study, LC_{50} determination revealed that (+)-IFZ exhibited marginally greater acute lethality compared to both rac-IFZ and (–)-IFZ. Morphological analysis further demonstrated that IFZ exposure induced significant swim bladder malformations in developing zebrafish larvae. The swim bladder is an important organ of zebrafish larvae, responsible for regulating buoyancy and assisting movement and breathing [21,22]. Abnormal development of the swim bladder, such as inflation failure, morphological deformity, or abnormal size, usually reflects abnormal development and impaired behavior and survival ability [23,24]. At the same time, it was observed that the pericardial area of larvae showed obvious blood pooling after IFZ exposure, suggesting that IFZ exposure could cause abnormal development and impaired function of the heart of zebrafish larvae [25]. Subsequently, the expression of genes involved in glucose metabolism, lipid metabolism, and apoptosis was quantified, along with physiological biomarkers including TG, TC, and glucose levels in the larvae. The results showed that TG levels increased significantly after IFZ exposure, and the expression of key genes for fatty acid β -oxidation, peroxisome proliferator-activated receptor alpha (*ppara*), and acyl-CoA oxidase (*aco*), was significantly downregulated after (+)-IFZ and (–)-IFZ exposure, which promoted lipid accumulation [26,27]. In addition, the expression of lipid synthesis-related genes 3-hydroxy-3-methylglutaryl-CoA reductase b (*hmgcrb*), acetyl-CoA carboxylase 1 (*acc1*), and fatty acid synthase (*fås*) was also significantly inhibited, which might be due to negative feedback regulation triggered by excessive lipid accumulation [28–30]. After rac-IFZ exposure, the expression of key enzyme gene glucose-6-phosphatase catalytic subunit a (*g6pca*) in the gluconeogenesis process and the rate-limiting enzyme gene glycogen phosphorylase I (*pygl*) in glycogenolysis was significantly upregulated, indicating that hepatic glucose output increased and glycogen reserves decreased [31]. After (+)-IFZ and (–)-IFZ exposure, the expression of pyruvate kinase (*pk*) and hexokinase 1 (*hk1*), key genes in the glycolysis process, was significantly downregulated, indicating that the glycolysis process was inhibited and glucose utilization was impaired [32]. Finally, the expression levels of apoptosis-related genes were measured and it was found that after IFZ exposure, the expression of the apoptosis-promoting gene bcl-2-associated x (*bax*) was upregulated,

and the expression of the apoptosis-inhibiting gene b-cell lymphoma 2 (*bcl2*) was significantly downregulated [33]. The significant increase in the *bax/bcl2* ratio indicated that IFZ exposure significantly promoted apoptosis. In summary, IFZ exposure was found to disrupt normal growth and development, impair glucose and lipid homeostasis, and promote apoptosis in zebrafish larvae.

As a model organism, zebrafish is extensively utilized in toxicological studies owing to its favorable characteristics, including embryonic transparency, rapid developmental cycles, and high genetic homology with mammals. Studies have shown that zebrafish embryos are highly sensitive to environmental pollutants, especially in terms of cardiac development, and are often used as an important model for evaluating cardiac toxicity [34,35]. As evident from Figure 1B, pronounced blood accumulation was observed within the pericardial region of the zebrafish larvae. The effect of IFZ on zebrafish cardiac development was investigated using cardiac transgenic zebrafish. IFZ exposure caused significant changes in cardiac-related parameters, and there were significant differences between (+)-IFZ and (–)-IFZ exposure, indicating that IFZ exposure affects zebrafish cardiac development and function. Ferrochelatase (FECH), the terminal enzyme in heme biosynthesis [36], is critical for endothelial cell proliferation in vitro and choroidal neovascularization in vivo [37]. Separately, fatty acid binding protein 3 (FABP3), a low-molecular-weight lipid chaperone, regulates lipid transport, metabolism, and transcriptional control [38,39]. Pathologically elevated FABP3 expression promotes cardiomyocyte apoptosis in myocardial infarct zones and border regions, worsening cardiac dysfunction through impaired left ventricular ejection fraction [40]. Hemoglobin subunit epsilon 1 (*hbbe1*) is a key marker gene related to cardiovascular development [41]. Tissue factor pathway inhibitor alpha (*tfpia*) is a negative regulator of coagulation in zebrafish and silencing it leads to thrombosis [42]. The changes in the above gene expression levels indicated that IFZ exposure could lead to abnormal cardiovascular development and cardiac function damage in zebrafish larvae, especially (+)-IFZ and (–)-IFZ exposure.

The liver plays a pivotal role in regulating lipid homeostasis, functioning as the primary site for multiple metabolic processes including fatty acid synthesis, lipid degradation, lipoprotein assembly and secretion, as well as the storage and mobilization of lipid droplets. It actively coordinates systemic lipid balance through the integration of hormonal and nutritional signals, thereby exerting profound effects on whole-body energy metabolism [43]. Our results indicated that exposure to IFZ led to substantial changes in the expression of genes associated with lipid metabolism (Figure 1C). To further examine IFZ's hepatic effects, we employed liver-specific transgenic zebrafish models. Quantitative analyses demonstrated that IFZ exposure increased liver size and disrupted antioxidant system homeostasis, with (+)-IFZ exhibiting more pronounced effects. These conclusions were supported by measurements of hepatic area, fluorescence intensity, and oxidative stress-related gene expression profiles in larvae.

Next, transcriptomic analysis was used to further explore the differences in toxic effects between rac-IFZ, (+)-IFZ and (–)-IFZ. The (–)-IFZ group had the largest number of DEGs, and in the PCA analysis result graph, it was the farthest from the CON group, indicating that (–)-IFZ exposure would lead to more significant differences. KEGG enrichment analysis was performed on the DEGs unique to each group. The analysis revealed predominant enrichment of lipid metabolism-associated pathways in the (+)-IFZ group, with the PPAR signaling pathway emerging as a pivotal transcriptional regulatory mechanism. This pathway plays a pivotal role in regulating lipid homeostasis, mediating inflammatory processes, and contributing to cardiovascular pathophysiology [44,45], indicating that (+)-IFZ mainly affects lipid metabolism in larvae. The (–)-IFZ group was mainly enriched in heart-related signaling pathways, among which adrenergic signaling

in cardiomyocytes regulates the response of cardiomyocytes to catecholamines such as epinephrine and norepinephrine, activates the $G\alpha_s$ -PKA pathway through β -adrenergic receptors (β -AR), and promotes glycogenolysis to provide energy support [46]. Retinol and its derivatives such as retinoic acid in retinol metabolism participate in the myocardial development process [47], indicating that (–)-IFZ mainly affected the heart development and function of larvae. The rac-IFZ exposure group exhibited significant enrichment in pathways associated with drug metabolism, with xenobiotic metabolism by cytochrome P450 enzymes, particularly involving CYP450 isoforms, serving as the central enzymatic system responsible for the biotransformation of foreign compounds [48]. Cytochrome P450 (CYP450), a heme-containing monooxygenase predominantly localized in the hepatic and extrahepatic endoplasmic reticulum [49], requires both NADPH coenzyme and molecular oxygen for its catalytic activity. This enzyme system primarily mediates the oxidative biotransformation of xenobiotics through various reactions including electron transfer, dehydrogenation, and oxygenation processes [50]. Studies have shown that triazole fungicides mainly inhibit the 14α -demethylation reaction mediated by fungal cytochrome P450, and block ergosterol synthesis, thereby destroying the cell membrane structure and exerting an antibacterial effect. This also showed that IFZ had the typical action characteristics of triazole fungicides.

To further compare the differences in toxic effects between (+)-IFZ and (–)-IFZ, transcriptomic analysis was performed on the DEGs of (+)-IFZ relative to (–)-IFZ, and GSEA analysis was performed on the four signaling pathways of fatty acid degradation, PPAR signaling pathway, adrenergic signaling in cardiomyocytes, and cardiac muscle contraction. The observed upregulation of both PPAR signaling and fatty acid degradation pathways suggested a coordinated activation of lipid metabolic processes, characterized by enhanced fatty acid β -oxidation and subsequent alterations in cellular energy homeostasis [51]. The observed enhancement of adrenergic signaling within cardiomyocytes, along with the potentiation of cardiac muscle contraction pathways, reflects a compensatory physiological response in juvenile fish. Under conditions of oxidative stress, this adaptive mechanism supports the maintenance of adequate organ perfusion through sympathetic nervous system activation and an increase in myocardial contractile force [52,53]. Furthermore, elevated heart rate and enhanced cardiac contractility resulted in greater ATP demand, triggering concurrent activation of fatty acid β -oxidation pathways to meet energy requirements.

While qPCR validation of selected genes can provide additional support for RNA-seq findings, the confirmation of transcriptome-based predictions derives from consistent phenotypic outcomes, such as hepatic developmental defects, compromised cardiac function, and altered expression of key genes, which directly reflect the biological impact of pathway dysregulation.

5. Conclusions

To evaluate the toxicity of IFZ enantiomers, zebrafish larvae were treated with rac-IFZ, (+)-IFZ, and (–)-IFZ. Developmental endpoints such as growth, cardiac and hepatic morphology, and organ function were subsequently assessed. The results revealed distinct enantiomer-specific toxicological profiles among the three treatments. Rac-IFZ, (+)-IFZ, and (–)-IFZ all significantly impaired larval growth and development, while (+)-IFZ and (–)-IFZ both significantly affected lipid metabolism and cardiac development and function. Subsequently, comparative transcriptome analysis was used to characterize enantiomer-specific gene expression profiles and identify distinct toxicological pathways among the three treatment groups, thereby elucidating the molecular mechanisms underlying their distinct phenotypic effects. The results revealed that rac-IFZ primarily disrupted drug metabolism pathways, (+)-IFZ preferentially altered lipid homeostasis, and (–)-IFZ exhibited cardiotoxicity, primarily affecting cardiac development and function. These findings

suggest that chiral configuration significantly influences the toxicological targets and outcomes of IFZ in developing zebrafish.

Author Contributions: Conceptualization, M.X.; Methodology, M.X.; Writing—original draft, M.X.; Investigation, Y.H.; Validation, Y.H.; Data curation, Y.H.; Supervision, M.Q., Y.J., and H.Z.; Writing—review & editing, M.Q., Y.J., and H.Z. All authors have read and agreed to the published version of the manuscript.

Funding: This research was funded by the National Natural Science Foundation of China (42277279) and Zhejiang Shuren University Scientific Reuter Foundation for Scholars (2021R040).

Institutional Review Board Statement: All experimental procedures, handling, use and care of the zebrafish used in this study regarding the protection of zebrafish used for scientific research purposes.

Informed Consent Statement: Not applicable.

Data Availability Statement: Data are available by contacting the authors.

Conflicts of Interest: The authors declare no conflicts of interest.

References

1. Ku, T.; Tan, X.; Liu, Y.; Wang, R.; Fan, L.; Ren, Z.; Ning, X.; Li, G.; Sang, N. Triazole fungicides exert neural differentiation alteration through H3K27me3 modifications: In vitro and in silico study. *J. Hazard. Mater.* **2023**, *459*, 132225. [[CrossRef](#)]
2. Ben Othmène, Y.; Monceaux, K.; Karoui, A.; Ben Salem, I.; Belhadef, A.; Abid-Essefi, S.; Lemaire, C. Tebuconazole induces ROS-dependent cardiac cell toxicity by activating DNA damage and mitochondrial apoptotic pathway. *Ecotox. Environ. Safe* **2020**, *204*, 111040. [[CrossRef](#)]
3. Roman, D.L.; Voiculescu, D.I.; Filip, M.; Ostafe, V.; Isvoran, A. Effects of Triazole Fungicides on Soil Microbiota and on the Activities of Enzymes Found in Soil: A Review. *Agriculture* **2021**, *11*, 893. [[CrossRef](#)]
4. Yang, Q.; Deng, P.; Xing, D.; Liu, H.; Shi, F.; Hu, L.; Zou, X.; Nie, H.; Zuo, J.; Zhuang, Z.; et al. Developmental Neurotoxicity of Difenconazole in Zebrafish Embryos. *Toxics* **2023**, *11*, 353. [[CrossRef](#)]
5. De la Paz, J.F.; Beiza, N.; Paredes-Zúñiga, S.; Hoare, M.S.; Allende, M.L. Triazole Fungicides Inhibit Zebrafish Hatching by Blocking the Secretory Function of Hatching Gland Cells. *Int. J. Mol. Sci.* **2017**, *18*, 710. [[CrossRef](#)]
6. Pamanji, R.; Ragothaman, P.; Koigoora, S.; Sivan, G.; Selvin, J. Network analysis of toxic endpoints of fungicides in zebrafish. *Toxicol. Res.* **2024**, *13*, tfae087. [[CrossRef](#)]
7. Yao, X.; Liang, C.; Lv, H.; Liu, W.; Wang, Q.; Ding, J.; Li, X.; Wang, J. Expanding the insight of ecological risk on the novel chiral pesticide mefentrifluconazole: Mechanism of enantioselective toxicity to earthworms (*Eisenia fetida*). *J. Hazard. Mater.* **2024**, *466*, 133585. [[CrossRef](#)]
8. Li, Y.; Ren, B.; Zhao, T.; Chen, H.; Zhao, Y.; Liang, H.; Liang, H. Enantioselective toxic effects of mefentrifluconazole in the early life stage of zebrafish (*Danio rerio*). *Environ. Toxicol.* **2022**, *37*, 1662–1674. [[CrossRef](#)] [[PubMed](#)]
9. Li, Y.; Liang, H.; Ren, B.; Zhao, T.; Chen, H.; Zhao, Y.; Liang, H. Enantioselective toxic effects of mefentrifluconazole in the liver of adult zebrafish (*Danio rerio*) based on transcription level and metabolomic profile. *Toxicology* **2022**, *467*, 153095. [[CrossRef](#)] [[PubMed](#)]
10. Zhang, H.; Wang, J.; Qian, M.; Jin, Y. Mefentrifluconazole exposure disrupted hepatic lipid metabolism disorder tightly associated with gut barrier function abnormal in mice. *Sci. Total Environ.* **2023**, *905*, 167317. [[CrossRef](#)]
11. Goldsmith, P. Zebrafish as a pharmacological tool: The how, why and when. *Curr. Opin. Pharmacol.* **2004**, *4*, 504–512. [[CrossRef](#)]
12. Hill, A.J.; Teraoka, H.; Heideman, W.; Peterson, R.E. Zebrafish as a model vertebrate for investigating chemical toxicity. *Toxicol. Sci.* **2005**, *86*, 6–19. [[CrossRef](#)]
13. Yadav, P.; Sarode, L.P.; Gaddam, R.R.; Kumar, P.; Bhatti, J.S.; Khurana, A.; Navik, U. Zebrafish as an emerging tool for drug discovery and development for thyroid diseases. *Fish Shellfish Immun.* **2022**, *130*, 53–60. [[CrossRef](#)]
14. Li, J.; Dong, C.; An, W.; Zhang, Y.; Zhao, Q.; Li, Z.; Jiao, B. Simultaneous Enantioselective Determination of Two New Isopropanol-Triazole Fungicides in Plant-Origin Foods Using Multiwalled Carbon Nanotubes in Reversed-Dispersive Solid-Phase Extraction and Ultrahigh-Performance Liquid Chromatography-Tandem Mass Spectrometry. *J. Agric. Food Chem.* **2020**, *68*, 5969–5979.
15. Fang, C.; Zhu, J.; Xu, H.; Qian, M.; Jin, Y. Polystyrene microplastics and cypermethrin exposure interfered the complexity of antibiotic resistance genes and induced metabolic dysfunction in the gut of adult zebrafish. *Environ. Pollut.* **2025**, *374*, 126288. [[CrossRef](#)]
16. Fang, C.; Di, S.; Zhang, Y.; Wang, X.; Jin, Y. 6PPD exposure reduced the melanin deposition by inhibiting tyrosinase activity in larval zebrafish. *Comp. Biochem. Physiol. C Toxicol. Pharmacol.* **2025**, *298*, 110300. [[CrossRef](#)] [[PubMed](#)]

17. Vanden Bossche, H.; Marichal, P.; Gorrens, J.; Coene, M.C. Biochemical basis for the activity and selectivity of oral antifungal drugs. *Br. J. Clin. Pract. Suppl.* **1990**, *71*, 41–46.
18. Wang, Y.; Ning, X.; Li, G.K.; Sang, N. New insights into potential estrogen agonistic activity of triazole fungicides and coupled metabolic disturbance. *J. Hazard. Mater.* **2022**, *424 Pt B*, 127479. [[CrossRef](#)] [[PubMed](#)]
19. Li, D.; Liu, M.Y.; Yang, Y.S.; Shi, H.H.; Zhou, J.L.; He, D.F. Strong lethality and teratogenicity of strobilurins on *Xenopus tropicalis* embryos: Basing on ten agricultural fungicides. *Environ. Pollut.* **2016**, *208*, 868–874. [[CrossRef](#)] [[PubMed](#)]
20. Busquet, F.; Strecker, R.; Rawlings, J.M.; Belanger, S.E.; Braunbeck, T.; Carr, G.J.; Ceni, P.; Fochtman, P.; Gourmelon, A.; Hubler, N.; et al. OECD validation study to assess intra- and inter-laboratory reproducibility of the zebrafish embryo toxicity test for acute aquatic toxicity testing. *Regul. Toxicol. Pharmacol.* **2014**, *69*, 496–511. [[CrossRef](#)]
21. Li, J.; Liang, Y.; Zhang, X.; Lu, J.; Zhang, J.; Ruan, T.; Zhou, Q.; Jiang, G. Impaired gas bladder inflation in zebrafish exposed to a novel heterocyclic brominated flame retardant tris(2,3-dibromopropyl) isocyanurate. *Environ. Sci. Technol.* **2011**, *45*, 9750–9757. [[CrossRef](#)] [[PubMed](#)]
22. Stinckens, E.; Vergauwen, L.; Ankley, G.T.; Blust, R.; Darras, V.M.; Villeneuve, D.L.; Witters, H.; Volz, D.C.; Knapen, D. An AOP-based alternative testing strategy to predict the impact of thyroid hormone disruption on swim bladder inflation in zebrafish. *Aquat. Toxicol.* **2018**, *200*, 1–12. [[CrossRef](#)]
23. Gao, Y.; Yang, P. The impaired swim bladder via ROS-mediated inhibition of the Wnt/Hedgehog pathway in zebrafish embryos exposed to eight toxic chemicals and binary chemical mixtures. *Chemosphere* **2023**, *338*, 139593. [[CrossRef](#)]
24. Price, E.R.; Mager, E.M. The effects of exposure to crude oil or PAHs on fish swim bladder development and function. *Comp. Biochem. Physiol. C Toxicol. Pharmacol.* **2020**, *238*, 108853. [[CrossRef](#)]
25. Kim, Y.; Jeon, H.J.; Kim, K.; Kim, C.; Moon, J.K.; Hwang, K.W.; Lee, S.E. Enantioselective effect of trifloxystrobin in early-stage zebrafish (*Danio rerio*) embryos: Cardiac abnormalities impacted by E,E-trifloxystrobin enantiomer. *Environ. Pollut.* **2023**, *327*, 121537. [[CrossRef](#)]
26. Qian, L.; Zhang, J.; Chen, X.; Qi, S.; Wu, P.; Wang, C.; Wang, C. Toxic effects of boscalid in adult zebrafish (*Danio rerio*) on carbohydrate and lipid metabolism. *Environ. Pollut.* **2019**, *247*, 775–782. [[CrossRef](#)]
27. Sun, L.; Li, J.; Zuo, Z.; Chen, M.; Wang, C. Chronic exposure to paclobutrazol causes hepatic steatosis in male rockfish *Sebastes marmoratus* and the mechanism involved. *Aquat. Toxicol.* **2013**, *126*, 148–153. [[CrossRef](#)] [[PubMed](#)]
28. Zhang, Z.F.; Song, T.T.; Chen, J.F.; Lv, G.Y. Recovery of a hypolipidemic polysaccharide from artificially cultivated *Sanguinaria officinalis* with an effective method. *Front. Nutr.* **2022**, *9*, 1095556. [[CrossRef](#)]
29. Zheng, Y.; Wang, Y.; Zheng, M.; Wang, G.; Zhao, H. Exposed to Sulfamethoxazole induced hepatic lipid metabolism disorder and intestinal microbiota changes on zebrafish (*Danio rerio*). *Comp. Biochem. Physiol. C Toxicol. Pharmacol.* **2022**, *253*, 109245. [[CrossRef](#)]
30. Fang, C.; Di, S.; Wang, C.; Hu, Q.; Jin, Y. Tire rubber-derived contaminant 6PPD had the potential to induce metabolism disorder in early developmental stage of zebrafish. *Comp. Biochem. Physiol. C Toxicol. Pharmacol.* **2025**, *287*, 110062.
31. Wang, L.; Lin, W.; Zha, Q.; Guo, H.; Zhang, D.; Yang, L.; Li, L.; Li, D.; Tang, R. Persistent Exposure to Environmental Levels of Microcystin-LR Disturbs Cortisol Production via Hypothalamic-Pituitary-Interrenal (HPI) Axis and Subsequently Liver Glucose Metabolism in Adult Male Zebrafish (*Danio rerio*). *Toxins* **2020**, *12*, 282. [[CrossRef](#)] [[PubMed](#)]
32. Liu, W.; He, Q.; Yue, C.; Xu, T.; Hang, X. Effects of dechlorane plus on hepatic pathology, metabolic health and gut microbiota in male mice. *Sci. Total Environ.* **2024**, *957*, 177532. [[CrossRef](#)]
33. Gaumer, S.; Guenal, I.; Brun, S.; Theodore, L.; Mignotte, B. Bcl-2 and Bax mammalian regulators of apoptosis are functional in *Drosophila*. *Cell Death Differ.* **2000**, *7*, 804–814. [[CrossRef](#)] [[PubMed](#)]
34. Stainier, D.Y. Zebrafish genetics and vertebrate heart formation. *Nat. Rev. Genet.* **2001**, *2*, 39–48. [[CrossRef](#)]
35. Verkerk, A.O.; Remme, C.A. Zebrafish: A novel research tool for cardiac (patho)electrophysiology and ion channel disorders. *Front. Physiol.* **2012**, *3*, 255. [[CrossRef](#)]
36. Ferreira, G.C.; Franco, R.; Lloyd, S.G.; Moura, I.; Moura, J.J.; Huynh, B.H. Structure and function of ferrocyclase. *J. Bioenerg. Biomembr.* **1995**, *27*, 221–229. [[CrossRef](#)]
37. Wijerathna, H.; Shanaka, K.; Raguvaran, S.S.; Jayamali, B.; Kim, S.H.; Kim, M.J.; Jung, S.; Lee, J. CRISPR/Cas9-Mediated *feh* Knockout Zebrafish: Unraveling the Pathogenesis of Erythropoietic Protoporphyrinuria and Facilitating Drug Screening. *Int. J. Mol. Sci.* **2024**, *25*, 10819. [[CrossRef](#)]
38. Bensaad, K.; Favaro, E.; Lewis, C.A.; Peck, B.; Lord, S.; Collins, J.M.; Pinnick, K.E.; Wigfield, S.; Buffa, F.M.; Li, J.L.; et al. Fatty acid uptake and lipid storage induced by HIF-1 α contribute to cell growth and survival after hypoxia-reoxygenation. *Cell Rep.* **2014**, *9*, 349–365. [[CrossRef](#)]
39. Shen, Y.; Song, G.; Liu, Y.; Zhou, L.; Liu, H.; Kong, X.; Sheng, Y.; Cao, K.; Qian, L. Silencing of FABP3 inhibits proliferation and promotes apoptosis in embryonic carcinoma cells. *Cell Biochem. Biophys.* **2013**, *66*, 139–146. [[CrossRef](#)]
40. Wu, S.; Kong, X.; Sun, Y.; Dai, X.; Yu, W.; Chen, R.; Ma, L.; Jiang, L. FABP3 overexpression promotes vascular fibrosis in Takayasu's arteritis by enhancing fatty acid oxidation in aorta adventitial fibroblasts. *Rheumatology* **2022**, *61*, 3071–3081. [[CrossRef](#)] [[PubMed](#)]
41. Chen, X.; Li, W. Isoflucypram cardiovascular toxicity in zebrafish (*Danio rerio*). *Sci. Total Environ.* **2021**, *787*, 147529. [[CrossRef](#)]

42. Raman, R.; Fallatah, W.; Qaryoute, A.A.; Ryon, M.; Jagadeeswaran, P. Knockdown and Knockout of Tissue Factor Pathway Inhibitor in Zebrafish. *Thromb. Haemost.* **2022**, *122*, 1104–1114. [[CrossRef](#)] [[PubMed](#)]
43. Jones, J.G. Hepatic glucose and lipid metabolism. *Diabetologia* **2016**, *59*, 1098–1103. [[CrossRef](#)]
44. Liu, W.; Wang, X.; Liu, Y.; Fang, S.; Wu, Z.; Han, C.; Shi, W.; Bao, Y. Effects of early florfenicol exposure on glutathione signaling pathway and PPAR signaling pathway in chick liver. *Ecotoxicol. Environ. Saf.* **2022**, *237*, 113529. [[CrossRef](#)] [[PubMed](#)]
45. Zou, J.; Song, Q.; Shaw, P.C.; Zuo, Z. Dendrobium officinale regulate lipid metabolism in diabetic mouse liver via PPAR-RXR signaling pathway: Evidence from an integrated multi-omics analysis. *Biomed. Pharmacother.* **2024**, *173*, 116395. [[CrossRef](#)]
46. Fu, Q.; Chen, X.; Xiang, Y.K. Compartmentalization of beta-adrenergic signals in cardiomyocytes. *Trends. Cardiovasc. Med.* **2013**, *23*, 250–256. [[CrossRef](#)]
47. Wu, Y.; Huang, T.; Li, X.; Shen, C.; Ren, H.; Wang, H.; Wu, T.; Fu, X.; Deng, S.; Feng, Z.; et al. Retinol dehydrogenase 10 reduction mediated retinol metabolism disorder promotes diabetic cardiomyopathy in male mice. *Nat. Commun.* **2023**, *14*, 1181. [[CrossRef](#)]
48. Zanger, U.M.; Schwab, M. Cytochrome P450 enzymes in drug metabolism: Regulation of gene expression, enzyme activities, and impact of genetic variation. *Pharmacol. Ther.* **2013**, *138*, 103–141. [[CrossRef](#)]
49. Guengerich, F.P. Mechanisms of Cytochrome P450-Catalyzed Oxidations. *ACS Catal.* **2018**, *8*, 10964–10976. [[CrossRef](#)] [[PubMed](#)]
50. Guengerich, F.P. Cytochrome p450 and chemical toxicology. *Chem. Res. Toxicol.* **2008**, *21*, 70–83. [[CrossRef](#)]
51. Mao, Z.; Feng, M.; Li, Z.; Zhou, M.; Xu, L.; Pan, K.; Wang, S.; Su, W.; Zhang, W. ETV5 Regulates Hepatic Fatty Acid Metabolism Through PPAR Signaling Pathway. *Diabetes* **2021**, *70*, 214–226. [[CrossRef](#)] [[PubMed](#)]
52. Mayourian, J.; Ceholski, D.K.; Gonzalez, D.M.; Cashman, T.J.; Sahoo, S.; Hajjar, R.J.; Costa, K.D. Physiologic, Pathologic, and Therapeutic Paracrine Modulation of Cardiac Excitation–Contraction Coupling. *Circ. Res.* **2018**, *122*, 167–183. [[CrossRef](#)] [[PubMed](#)]
53. Papa, A.; Kushner, J.; Marx, S.O. Adrenergic Regulation of Calcium Channels in the Heart. *Annu. Rev. Physiol.* **2022**, *84*, 285–306. [[CrossRef](#)] [[PubMed](#)]

Disclaimer/Publisher’s Note: The statements, opinions and data contained in all publications are solely those of the individual author(s) and contributor(s) and not of MDPI and/or the editor(s). MDPI and/or the editor(s) disclaim responsibility for any injury to people or property resulting from any ideas, methods, instructions or products referred to in the content.